

Supplemental Data

A single glycine in extracellular loop 1 is the critical determinant for pharmacological specificity of dopamine D2 and D3 receptors

Mayako Michino, Prashant Donthamsetti, Thijs Beuming, Ashwini Banala, Lihua Duan,

Thomas Roux, Yang Han, Eric Trinquet, Amy Hauck Newman, Jonathan A. Javitch, Lei Shi

Department of Physiology and Biophysics and Institute for Computational Biomedicine, Weill Medical College of Cornell University, New York, New York (M.M., L.S.); Departments of Psychiatry and Pharmacology, Columbia University College of Physicians and Surgeons, and Division of Molecular Therapeutics, New York State Psychiatric Institute, New York, New York (P.D., L.D., Y.H., J.A.J.); Schrödinger Inc., New York, New York (T.B.); Medicinal Chemistry Section, Molecular Targets and Medications Discovery Branch, National Institute on Drug Abuse - Intramural Research Program, Baltimore, Maryland (A.B., A.H.N.); Cisbio Bioassays, Codolet, France (T.R., E.T.).

Article submitted to the journal: **Molecular Pharmacology**

Synthesis

***N*-(3-(4-(2,3-dichlorophenyl)piperazin-1-yl)propyl)-1*H*-indole-2-carboxamide (C3; BAK-04-62)** was prepared using the amide coupling reagent, CDI (778 mg, 4.8 mmol) that was added to a solution of 1*H*-indole-2-carboxylic acid (773 mg, 4.8 mmol) in THF (10 mL). The resulting mixture was stirred at RT for 2 h. The solution was cooled to 0 °C and 3-(4-(2,3-dichlorophenyl)piperazin-1-yl)propan-1-amine (Robarge et al., 2001) (1.3 g, 4.8 mmol) in THF (10 mL) was added drop wise. The reaction mixture was allowed to warm to RT and stirred for 2-3 h. The reaction mixture was concentrated and the crude product was recrystallized from 2-propanol. Yield: 74% (1.53 g). Mp >250 °C (HCl salt); ¹H NMR (400 MHz, DMSO) δ 11.54 (brs, 1H), 8.48 (t, *J* = 5.2 Hz, 1H), 7.59 (d, *J* = 7.6 Hz, 1H), 7.42 (d, *J* = 8.4 Hz, 1H), 7.30-7.28 (m, 2H), 7.18-7.09 (m, 3H), 7.02 (t, *J* = 7.2 Hz, 1H), 3.34 (t, *J* = 6.4 Hz, 2H), 2.99 (brs, 4H), 2.55 (brs, 4H), 2.43 (t, *J* = 6.8 Hz, 2H), 1.77-1.74 (m, 2H); ¹³C NMR (100 MHz, CDCl₃) δ 161.67, 151.23, 136.33, 134.30, 131.59, 127.85, 127.75, 127.71, 125.07, 124.36, 121.75, 120.70, 118.70, 112.20, 101.93, 58.43, 53.65, 51.58, 40.54, 24.75; Anal. (C₂₂H₂₄Cl₂N₄O·HCl·1/4H₂O) C, H, N.

***N*-(5-(4-(2,3-dichlorophenyl)piperazin-1-yl)pentyl)-1*H*-indole-2-carboxamide (C5; BAK-04-66)** was prepared by a similar method described for BAK-04-62 employing 1*H*-indole-2-carboxylic acid and 5-(4-(2,3-dichlorophenyl)piperazin-1-yl)hexan-1-amine (Robarge et al., 2001). Yield: 72% (2.8 g). Mp 218-219 °C (oxalate salt); ¹H NMR (400 MHz, CDCl₃) δ 9.40 (brs, 1H), 7.64 (d, *J* = 7.6 Hz, 1H), 7.44 (d, *J* = 8.0 Hz, 1H), 7.31-7.26 (m, 1H), 7.16-7.14 (m, 3H), 6.92 (dd, *J* = 7.2, 1.6 Hz, 1H), 6.82 (d, *J* = 2.0 Hz, 1H), 6.20 (t, *J* = 5.6 Hz, 1H), 3.52 (q, *J* = 6.4 Hz, 2H), 3.05 (brs, 4H), 2.62 (brs, 4H), 2.43 (t, *J* = 7.2 Hz, 2H), 1.73-1.56 (m, 4H), 1.50-1.42 (m, 2H); ¹³C NMR (100 MHz, CDCl₃) δ 161.98, 151.41, 136.60, 134.06, 130.98, 127.70, 127.54, 124.58, 124.42, 121.91, 120.64, 118.68, 112.24, 101.86, 58.48, 53.41, 51.40, 39.78, 29.81, 26.63, 24.96; Anal. (C₂₄H₂₈Cl₂N₄O·C₂H₂O₄·2/5H₂O) C, H, N.

Supplemental Table 1. List of MD simulations. Multiple MD trajectories were collected for each receptor-ligand complex, and numbered sequentially. The initial and final binding modes of the SP within the SBP are indicated as follows: *Ptm23*, SP is in the Ptm23 sub-pocket; *Ptm27*, SP is in the Ptm27 sub-pocket; *Ptm23'*, SP is in the Ptm23 sub-pocket, but not tightly associated; *exposed*, SP is extensively exposed to the extracellular milieu (see Supplemental Fig. 2). The dominant final SP poses are highlighted in bold.

Receptor	Ligand	Trajectory Index	Simulation length (ns)	Initial SP pose	Final SP pose
D3R	R-22	1	18	Ptm27	exposed
		2	18	Ptm27	Ptm23
		3	24	Ptm27	Ptm23
		4	18	Ptm27	Ptm23
		5	18	Ptm23	Ptm23
		6	18	Ptm23	Ptm23
	C4	1	18	Ptm23	exposed
		2	18	Ptm23	Ptm23
		3	18	Ptm23	Ptm23
	C3	1	18	Ptm23	Ptm23'
		2	24	Ptm23	Ptm23'
		3	18	Ptm27	Ptm23
	C5	1	18	Ptm23	Ptm23
		2	18	Ptm23	Ptm23
	D2R	R-22	1	24	Ptm27
2			18	Ptm27	Ptm27
3			18	Ptm27	Ptm27
4			24	Ptm27	Ptm27
C4		1	18	Ptm27	Ptm27
		2	18	Ptm27	Ptm27
		3	24	Ptm27	Ptm27
C3		1	18	Ptm23	Ptm23'
		2	18	Ptm27	exposed
		3	18	Ptm23	Ptm23'
C5		1	18	Ptm27	Ptm27
		2	18	Ptm27	Ptm27
		3	18	Ptm27	exposed

Supplemental Table 2. List of REMD simulations. Multiple REMD trajectories were collected for each receptor-ligand complex, and numbered sequentially. The initial SP pose indicates the binding mode of SP within the SBP in the starting conformations of the simulation and the final SP pose indicates the binding mode of SP within the SBP in the last 0.96 ns of 310 K ensemble (See Supplemental Table 1 and Supplemental Fig. 2 for the classification of binding modes). The population frequency of a particular binding mode is shown in parentheses. The dominant final SP poses are highlighted in bold.

Receptor	Ligand	Trajectory Index	Number of replicas	Temperature range (K)	Simulation Length (ns)	Average acceptance ratio	Initial SP Pose(s)	Final SP Pose(s)
D3R	R-22	1	14	310-333	10.32	0.15	Ptm27	Ptm23 (0.83) , Ptm27 (0.17)
		2	14	310-333	4.56	0.14	Ptm27	Ptm23 (0.875) , Ptm27 (0.125)
		3	18	310-333.2	8.4	0.26	Ptm27	Ptm23 (0.55) , exposed (0.163), Ptm27 (0.287)
	C3	1	18	310-333.2	7.68	0.26	Ptm23'	Ptm23 (0.075), Ptm23' (0.925)
		2	18	310-333.2	6.48	0.26	Ptm23 (0.5), Ptm23' (0.5)	Ptm23' (1.0)
	C5	1	18	310-333.2	5.76	0.26	Ptm23	Ptm23 (1.0)
D2R	R-22	1	14	310-333	4.8	0.16	Ptm27	Ptm27 (1.0)
		2	14	310-333	4.56	0.16	Ptm27	Ptm27 (1.0)
	C3	1	18	310-333.2	13.44	0.27	Ptm27	Ptm23' (0.29) , exposed (0.71)
		2	18	310-333.2	7.68	0.27	Ptm23 (0.5), Ptm27 (0.5)	Ptm23' (0.963) , exposed (0.037)
	C5	1	18	310-333.2	9.6	0.27	Ptm23 (0.5), Ptm27 (0.5)	Ptm23' (0.65), exposed (0.35)

Supplemental Table 3. Analysis of distances between the SP and the Ptm23 sub-pocket in D3R/R-22 vs D3R/C3. The distances from the center of mass of the SP indole ring to C α atoms of individual (V86^{2.61}, L89^{2.64}, F106^{3.28}, G94, C181) and subsets of residues ('Ptm23_3': V86^{2.61}, L89^{2.64}, F106^{3.28}; 'Ptm23_4': V86^{2.61}, L89^{2.64}, F106^{3.28}, C181; 'Ptm23_5': V86^{2.61}, L89^{2.64}, F106^{3.28}, G94, C181) in the Ptm23 sub-pocket were measured for the D3R in complex with R-22 and the C3 analog. The distances were measured in the frames from MD (last 100 frames, 2.4 ns) and REMD (clusters within last 80 frames, 0.96 ns) simulations with the converged ligand poses (highlighted in bold in Supplemental Tables 1 and 2), and averaged for each trajectory. The average across all trajectories of D3R/R-22 and D3R/C3 are shown in the 'average' rows, and the values marked with * indicate that they differ by > 1 Å between R-22 and C3.

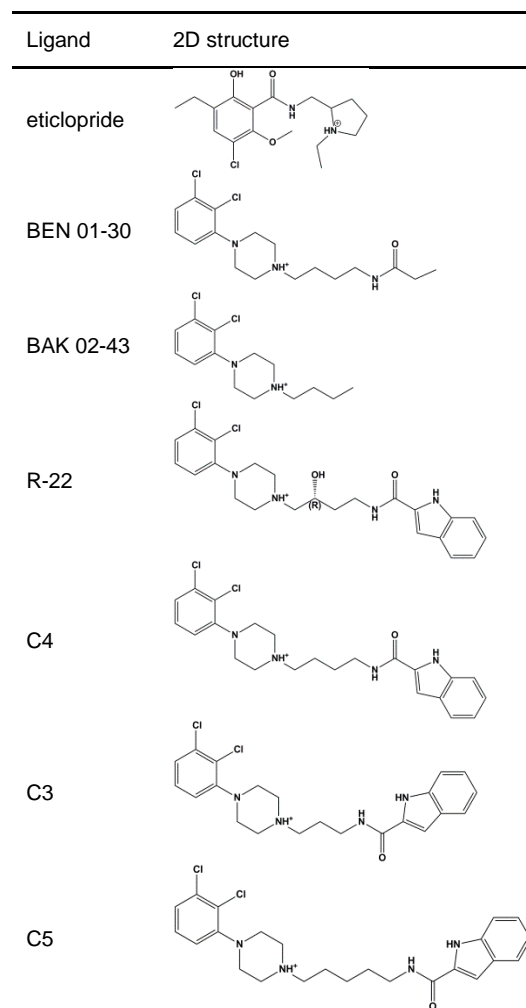
Ligand	Traj. Index	V86 ^{2.61}	L89 ^{2.64}	F106 ^{3.28}	G94	C181	Ptm23_3	Ptm23_4	Ptm23_5
R-22	MD 2	5.6	6.1	9.9	6.5	5.7	4.7	3.6	2.6
	MD 3	5.6	5.9	10.7	5.8	7.1	5.4	4.7	3.9
	MD 4	5.7	5.2	11.5	5.2	8.4	5.7	5.5	4.6
	MD 5	5.6	6.3	10.3	6.6	5.6	4.8	3.7	2.7
	MD 6	5.8	5.9	10.0	6.3	5.5	5.0	3.7	2.6
	REMD 1	6.1	6.0	11.4	5.6	7.2	5.9	5.3	4.4
	REMD 2	7.5	5.9	12.7	4.3	7.5	7.4	6.6	5.5
	REMD 3	8.0	7.0	12.1	4.8	6.4	7.3	6.2	5.1
	average	6.2	6.0*	11.1*	5.7*	6.7*	5.8	4.9	3.9
C3	MD 1	7.7	8.2	9.7	7.4	4.4	6.4	4.8	4.2
	MD 2	4.6	6.8	11.0	7.8	6.4	5.3	4.6	3.6
	REMD 1	6.9	8.2	9.7	7.2	4.6	5.9	4.4	3.8
	REMD 2	7.4	8.0	9.6	7.2	4.4	6.1	4.6	4.0
	average	6.6	7.8*	10.0*	7.4*	4.9*	5.9	4.6	3.9

Supplemental Table 4. Analysis of the Prokink associated with Pro^{2.59}. The Prokink parameters (bend angle, wobble angle, and face shift angle) of Pro^{2.59} were measured for the D2R and D3R in complex with the indicated compounds. For eticlopride, the angles were calculated for both the crystal structure (PDB: 3PBL), and the frames from MD simulations (36 ns for each of the D2R/eticlopride and D3R/eticlopride MD simulations); for all other ligands, the angles were calculated based on the frames from MD and REMD trajectories with the converged ligand poses (highlighted in bold in Supplemental Tables 1 and 2). The average values of the angles are shown. The angles marked with * differ from the angles in the eticlopride-bound complex of the same receptor by > 15 degrees.

Receptor	Ligand	Bend angle	Wobble angle	Face shift
D3	eticlopride (PDB: 3PBL)	32.4	-51.8	106.4
	eticlopride	31.4	-49.9	114.2
	BEN 01-30 ^a	30.1	-52.4	109.9
	BAK 02-43 ^b	31.9	-56.8	113.9
	R-22	26.7	-66.9*	105.3
	C4	37.6	-67.4*	115.4
	C3	26.8	-50.8	112.1
D2	C5	26.7	-69.5*	107.3
	eticlopride	31.3	-48.1	115.0
	R-22	28.8	-43.6	111.8
	C4	29.8	-47.3	116.1
	C3	30.5	-41.4	113.0
C5	32.3	-34.7	111.6	

^a N-(4-(4-(2,3-Dichlorophenyl)piperazin-1-yl)butyl)propionamide (Banala et al., 2011)

^b 1-Butyl-4-(2,3-dichlorophenyl)piperazine (Newman et al., 2012)



Supplemental Table 5. Radioligand membrane binding affinities of NAPS and R-22 at selected chimera and mutant constructs

	NAPS				R-22			
	pK _i	S.E.M.	Fold affinity increase (relative to D2R wildtype)	Fold affinity decrease (relative to D3R wildtype)	pK _i	S.E.M.	Fold affinity increase (relative to D2R wildtype)	Fold affinity decrease (relative to D3R wildtype)
D3R	9.26	0.06	0.6	1.0	9.02	0.07	157.2	1.0
D3R(Δ 94G)	9.54	0.06		0.5	7.33 ^{σ}	0.17		49.3
D2R_D3R(EL1)	9.68	0.07	1.7		8.38 ^{σ}	0.05	35.9	
D2R_D3R(EL2)	9.28	0.06	0.7		6.89 ^{γ}	0.06	1.2	
D2R_D3R(EL1_EL2)	9.59	0.08	1.3		8.63 ^{δ}	0.11	64.2	
D2R(98-99GGE)	9.27	0.11	0.6		8.09 ^{σ}	0.05	18.4	
D2R	9.47	0.04	1.0	0.6	6.82	0.01	1.0	157.2

Statistical significance was determined by one-way ANOVA with Bonferroni post hoc test.

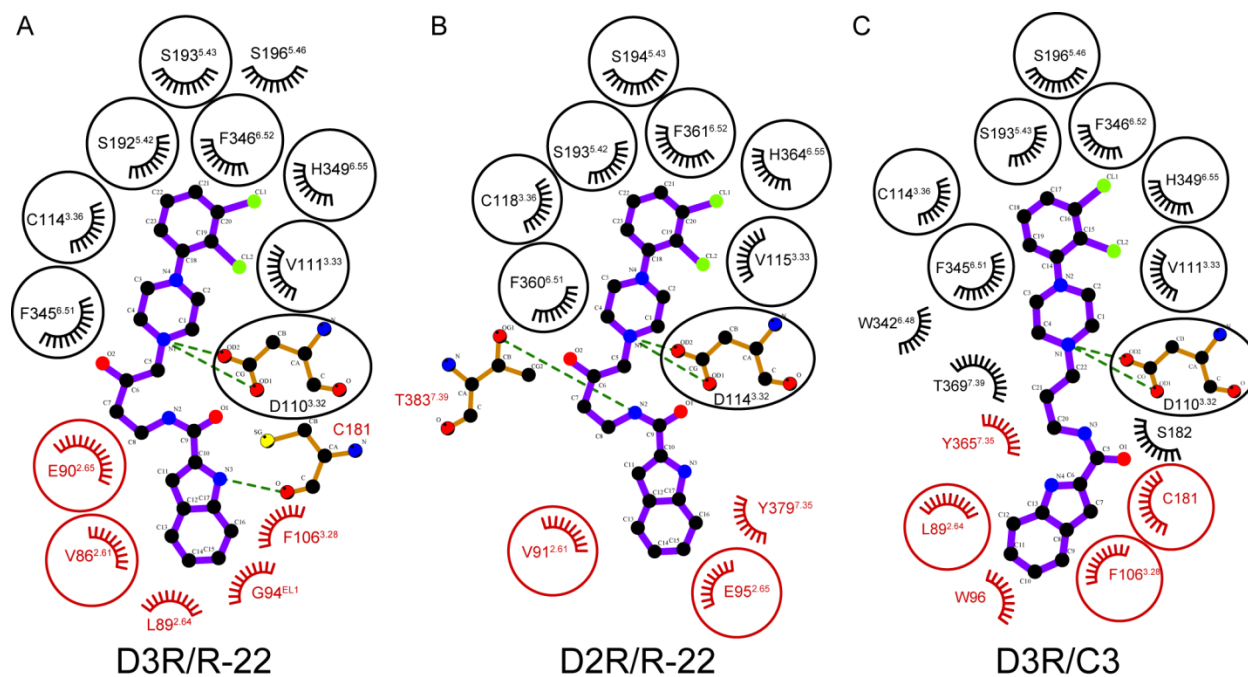
None of the mutations significantly altered the pK_i values for NAPS ($p > 0.1$).

For R-22, ^{γ} indicates that the pK_i is significantly different from that at D3R ($p < 0.05$) but not at D2R ($p > 0.5$), ^{δ} indicates that the pK_i is significantly different from that at D2R ($p < 0.05$) but not at D3R ($p > 0.5$), whereas ^{σ} indicates that the pK_i is significantly different from that at D2R ($p < 0.05$) but also at D3R ($p < 0.05$).

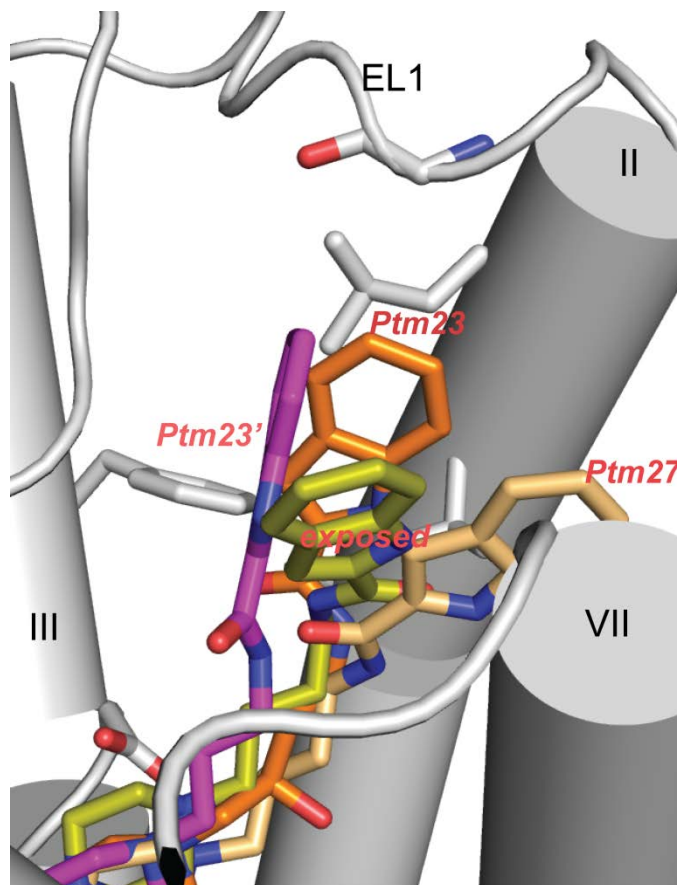
Supplemental Table 6. Radioligand whole cell binding affinities of NAPS and R-22 at wildtype constructs

	D2R		D3R		D2R/D3R
	pK _i	S.E.M.	pK _i	S.E.M.	
NAPS	9.41	0.20	9.02	0.09	0.41
R-22	6.81	0.07	8.48	0.08	47.79

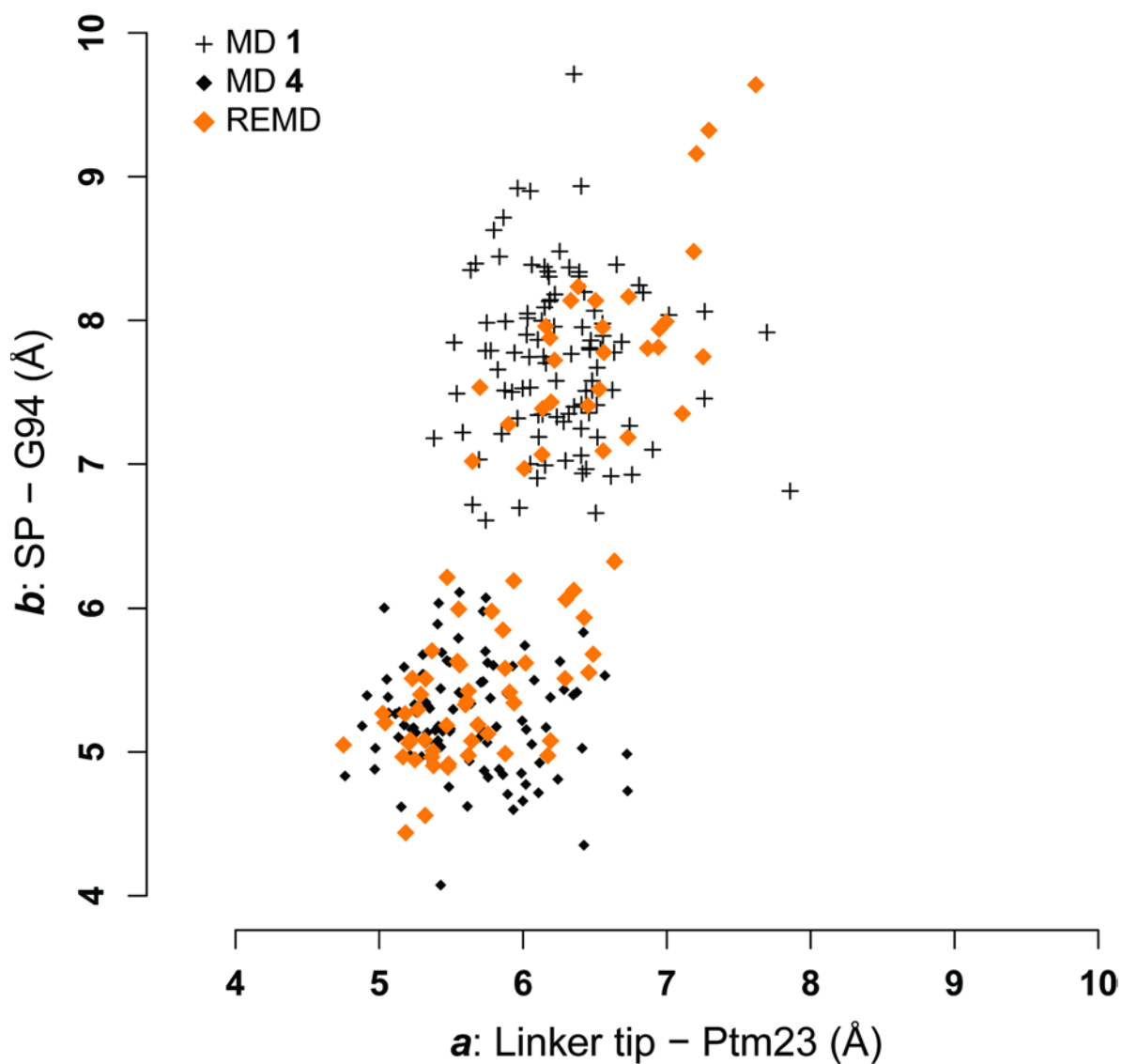
Supplemental Figure 1. Receptor-ligand interactions of R-22 in D3R and D2R, and C3 in D3R. The residues shown (red: interacting with the SP moiety or the linker; black: interacting with the PP) are within 4.0 Å of the ligand heavy atom in >80% of last 100 frames (2.4 ns) pooled from selected MD trajectories of D3R/R-22, D2R/R-22, and D3R/C3. The circled residues in D3R/R-22 and D2R/R-22 are the common residues between the two complexes. The circled residues in D3R/C3 are those common with D3R/R-22. The diagrams were prepared with LigPlot+ (Laskowski and Swindells, 2011), and modified according to the residue interaction statistics in the simulations. The ligands R-22 and C3 are shown in 2D with purple bonds between atoms represented in filled circles; the hydrogen bonds are shown in green dashed lines; the hydrophobic contacts are shown as spoked arcs.



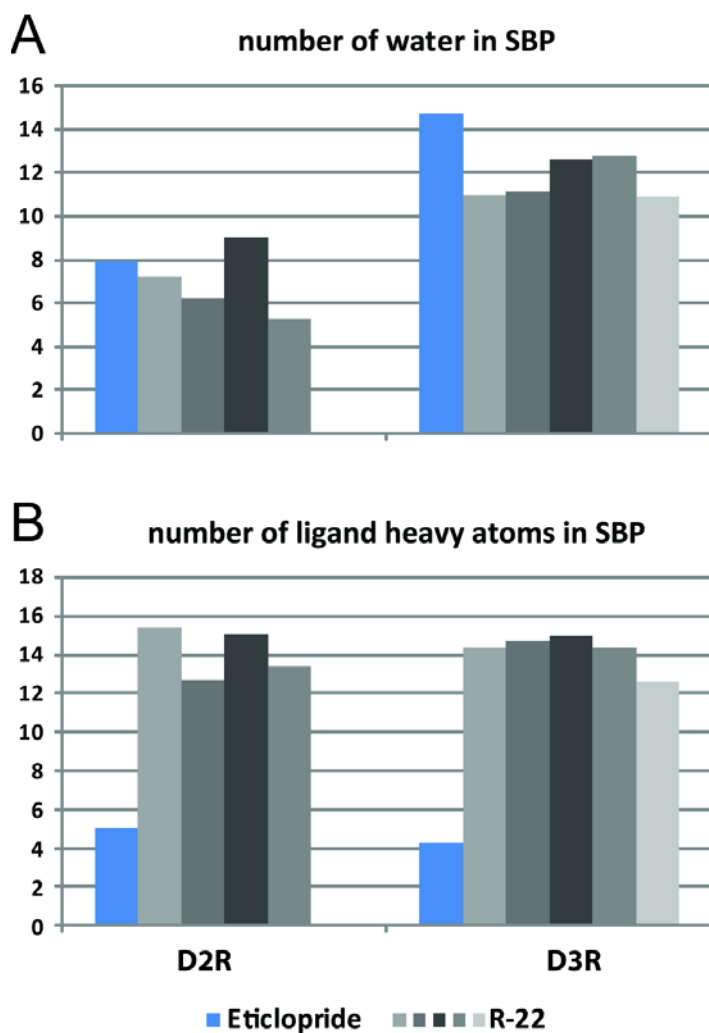
Supplemental Figure 2. The binding mode of SP within the SBP can be categorized into four types of poses: *Ptm23* (orange), SP is in the Ptm23 pocket; *Ptm27* (light orange), SP is in the Ptm27 pocket; *Ptm23'* (magenta), SP is in the Ptm23 pocket, but not tightly associated; *exposed* (yellow), SP is extensively exposed to the extracellular milieu. The R-22-bound D3R model is shown in gray, and all other receptor models are not shown for clarity. The *Ptm23* pose is well-defined, and can be characterized by interaction with residues V86^{2.61}, L89^{2.64}, G94 (EL1), F106^{3.28}, and Cys181 (EL2). The other three poses are less well-defined in space, but are still distinct from each other.



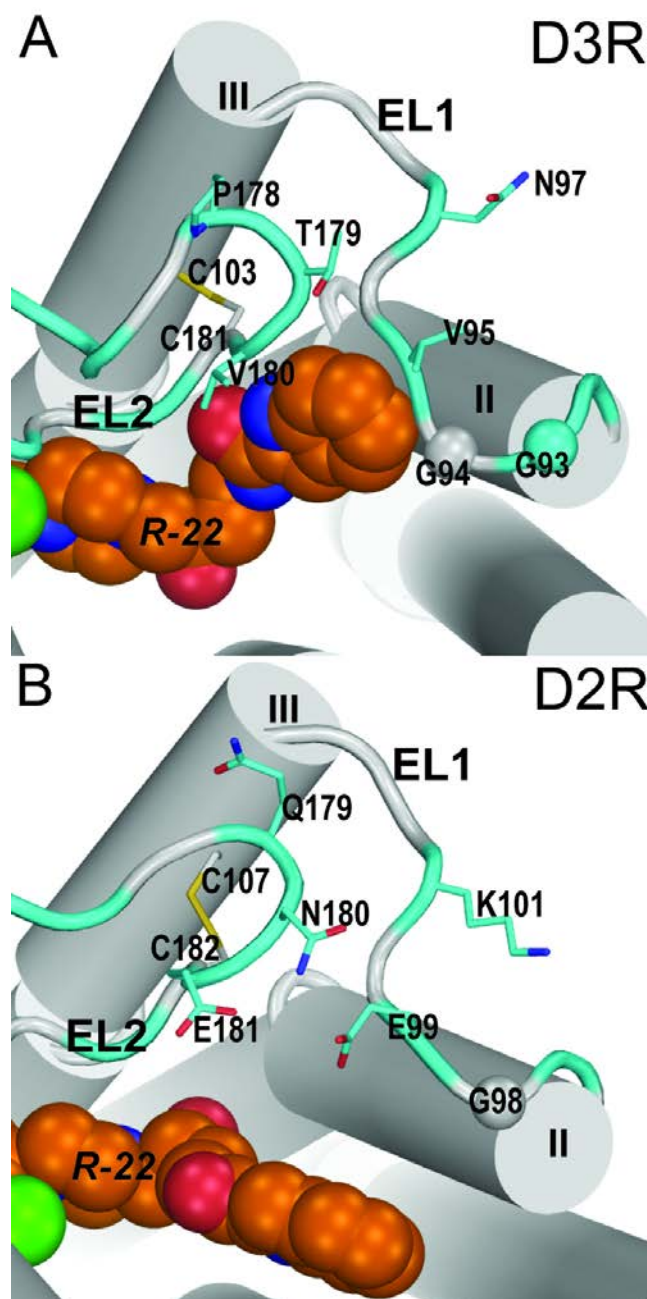
Supplemental Figure 3. A scatterplot of the D3R/R-22 receptor-ligand distances (MD 1 in black crosses, MD 4 in black diamonds, and REMD 1 in orange diamonds) shows greater sampling of ligand conformations in REMD compared to the regular MD, as the distance space covered by one REMD trajectory is larger than that covered by any one of the MD trajectories. The distance measurements are taken from the last 2.4 ns for the MD simulations and the last 0.96 ns of the 310 K ensemble for the REMD simulations.



Supplemental Figure 4. The number of water molecules in the SBP (**A**), and the number of ligand heavy atoms in the SBP (**B**) are shown for D3R and D2R in complex with R-22 (gray bars for D3R/R-22 MD 2-6 and D2R/R-22 MD 1-4) and eticlopride (blue bars). Each bar is an average count from all frames in a single MD trajectory. Significantly larger number of water molecules is found in the SBP of D3R/R-22 than in D2R/R-22 (t-test p-value < 0.0005). The average number of water molecules found across multiple trajectories is 11.7 (\pm 0.9) for D3R/R-22 and 6.9 (\pm 1.6) for D2R/R-22.



Supplemental Figure 5. Divergent EL1-EL2 interfaces in D3R (A) and D2R (B). The residues that form the EL1-EL2 interface are divergent in both electrostatic properties (the presence of three charged residues Glu99, Lys101, and Glu181 in D2R but not in D3R) and rigidity (Pro178 in D3R compared to Q179 in D2R). As a result, Gly94 of D3R is oriented toward the SBP, while Gly98 of D2R is oriented toward Ptm27. The divergent positions are highlighted by cyan.



References

- Banala AK, Levy BA, Khatri SS, Furman CA, Roof RA, Mishra Y, Griffin SA, Sibley DR, Luedtke RR and Newman AH (2011) N-(3-fluoro-4-(4-(2-methoxy or 2,3-dichlorophenyl)piperazine-1-yl)butyl)arylcarboxamides as selective dopamine D3 receptor ligands: critical role of the carboxamide linker for D3 receptor selectivity. *J Med Chem* **54**(10): 3581-3594.
- Laskowski RA and Swindells MB (2011) LigPlot+: multiple ligand-protein interaction diagrams for drug discovery. *J Chem Inf Model* **51**(10): 2778-2786.
- Newman AH, Beuming T, Banala AK, Donthamsetti P, Pongetti K, LaBounty A, Levy B, Cao J, Michino M, Luedtke RR, Javitch JA and Shi L (2012) Molecular determinants of selectivity and efficacy at the dopamine D3 receptor. *J Med Chem* **55**(15): 6689-6699.
- Robarge MJ, Husbands SM, Kieltyka A, Brodbeck R, Thurkauf A and Newman AH (2001) Design and synthesis of [(2,3-dichlorophenyl)piperazin-1-yl]alkylfluorenylcarboxamides as novel ligands selective for the dopamine D3 receptor subtype. *J Med Chem* **44**(19): 3175-3186.